mathematics

MDPI

Article

Solution Properties of a New Dynamic Model for MEMS with Parallel Plates in the Presence of Fringing Field

Paolo Di Barba [1], Luisa Fattorusso [2] and Mario Versaci [3,*]

[1] Dipartimento di Ingegneria Industriale e dell'Informazione, University of Pavia, Via A. Ferrata 5, I-27100 Pavia, Italy
[2] Dipartimento di Ingegneria dell'Informazione Infrastrutture Energia Sostenibile, "Mediterranea" University, Via Graziella Feo di Vito, I-89122 Reggio Calabria, Italy
[3] Dipartimento di Ingegneria Civile Energia Ambiente e Materiali, "Mediterranea" University, Via Graziella Feo di Vito, I-89122 Reggio Calabria, Italy
* Correspondence: mario.versaci@unirc.it; Tel.: +39-09651692273

Abstract: In this paper, starting from a well-known nonlinear hyperbolic integro-differential model of the fourth order describing the dynamic behavior of an electrostatic MEMS with a parallel plate, the authors propose an upgrade of it by formulating an additive term due to the effects produced by the fringing field and satisfying the Pelesko–Driscoll theory, which, as is well known, has strong experimental confirmation. Exploiting the theory of hyperbolic equations in Hilbert spaces, and also utilizing Campanato's Near Operator Theory (and subsequent applications), results of existence and regularity of the solution are proved and discussed particularly usefully in anticipation of the development of numerical approaches for recovering the profile of the deformable plate for a wide range of applications.

Keywords: MEMS with deformable plate; hyperbolic dimensionless fourth-order integro-diffferential dynamic model; nonlinearities; Pelesko–Driscoll's approach for fringing field modeling; Campanato's near operator theory

MSC: 35A01; 35A02; 35Q99; 35R09

Citation: Di Barba, P.; Fattorusso, L.; Versaci, M. Solution Properties of a New Dynamic Model for MEMS with Parallel Plates in the Presence of Fringing Field. *Mathematics* **2022**, *10*, 4541. https://doi.org/10.3390/math10234541

Academic Editor: André Nicolet

Received: 2 November 2022
Accepted: 25 November 2022
Published: 1 December 2022

1. Introduction

In recent years, physical-mathematical scientific research has produced complete analytical models capable of simulating the behavior of parallel plate MEMS (micro-electro-mechanical systems) characterized by strong confirmation with experimental evidence [1–4]. Particularly, a wide range of models of electrostatic actuators, obtained through refined design techniques, have been developed for several applications [5,6], including MEMS-based metamaterial [7,8]. This has made it possible to highlight a strong synergy between undoubted theoretical skills and industrial realities by carrying out technological transfers that were previously prohibitive [9–11], also with manufacturing imperfections (which, notoriously, affect the operation of MEMS devices), if taken into account during the modeling and design phases [12,13] (i.e., by means of asymptotic homogenization techniques [14]). These devices, nowadays, considered "intelligent", are able to combine electrical, electronic, mechanical, and optical effects by managing highly complex industrial processes [15–20], especially when nonlinear dynamic characteristics of MEMS devices are involved, so that the relative simulation accuracy is low and cannot meet the needs of design applications [21,22]. Modern industrial technologies allow the production of micro-products, even with complex geometries, in which the deformable elements take on particular connotations and characteristics. Among them, the electrostatic MEMS (in which the deformable element is a metal plate) stand out since they do not have particular precautions for their construction and exhibit high-level performance [1,23–25]. Moreover, for many of them, it was possible

to study their behavior even with deformable elements initially curved and loaded by nonlinear electrostatic actions to study, using completely innovative techniques, any instability and/or bistability [26–28]. Today, scientific research works hard in proposing advanced physical-mathematical models with the primary objective of producing synergies with industrial research through possible correspondences with experimental models [29–32]. Obviously, regardless of the intended use of the device, it is imperative that the deformable element inside it does not come into contact with the fixed elements (to avoid the generation of highly harmful electrostatic discharges) [33–35], avoiding any very dangerous instability in several applications (in such cases, one needs to exploit special techniques able to also recover the stability regions [36,37]). Therefore, it is imperative to limit the physical causes behind the excessive deformation of the deformable element [10,38]. Among them, the capacitive fringing field is one of the most frequent causes of instability of electrostatic MEMS devices [39,40]. As is known, it depends on the geometry of the device (in particular on its length/width ratio, L/d) producing in the device harmful effects on the bending of the lines of force of **E** [41,42], and it is important to highlight that this influence is stronger near the edges, while it is considered to be negligible in the center [43–46].

In the recent past, the authors have produced scientific works of modeling of electrostatic MEMS devices for industrial and biomedical applications, as well as of recovering the profile of the deformable element by means of numerical techniques, where the deformable element was a membrane. Particularly, a second order semi-linear elliptical model was developed and studied (in the absence or presence of a fringing field, with amplitude of the electric field locally proportional to the curvature of the membrane [47]), which, by applying "ad-hoc" numerical procedures, produced recovery of the membrane profile fully consistent with the experimental evidence [10,48,49]. In parallel, the authors became interested in modeling MEMS devices with parallel plates. In particular, starting from a well-known fourth order integro-differential model [50] of general validity for electrostatic MEMS devices with parallel plates, they reformulated the problem in the presence of fringing fields obtaining results of existence and uniqueness of the solution [3], from which to recover the profile of the deformable element using numerical techniques [51]. However, these models proposed and studied by the authors do not also present, up to now, dynamic components.

Concerning electrostatic MEMS devices with parallel plates, an important dynamic dimensionless integro-differential dynamic model (of the fourth order) has been studied in detail in [52], where important existence and regularity results for the solution (profile of the deformable plate) have been demonstrated in the absence of the fringing field, offering interesting food for thought regarding potential future developments. Particularly, in [52], it was considered

$$\begin{cases} \Delta^2 u(x,t) + c(x,t)u'(x,t) + u''(x,t) = \\ G(\beta,\gamma,u) + H(\lambda(t),\chi,\delta(x,t),p(x),u(x,t)), \quad \text{in } \Omega\times[0,T), \\ 0 \le u(x,t) < 1, \quad \text{in } \Omega\times[0,T] \quad x\in\Omega\subset\mathbb{R}^N, \quad 1\le N<4, \\ u(x,t) = 0, \quad \text{on } \partial\Omega\times[0,T], \\ \nabla u(x,t) - d\frac{\partial u(x,t)}{\partial \nu} = 0, \quad \text{on } \partial\Omega\times[0,T], \end{cases} \tag{1}$$

where

1. x is the spatial variable, while t is the time variable;
2. $\Omega\subset\mathbb{R}^N$, $\le N\le 3$ represents a bounded domain with a sufficiently smooth boundary (i.e., the device electrostatic MEMS with a deformable plate under study);
3. $u(x,t)$ is the profile of the deformable plate;
4. $'$ represents the derivative with respect to time;
5. ν is the outward pointing normal to $\partial\Omega$;
6. $c(x,t)$ is a bounded real function that is related to anisotropic damping phenomena;

7.
$$G(\beta,\gamma,u) := -\Big(\beta\int_\Omega |\nabla u(x,t)|^2 \mathrm{dx} + \gamma\Big)\Delta u(x,t), \tag{2}$$
in which γ is a positive dimensionless parameters linked to the stretching effect in the deformable plate while β (also positive and dimensionless) takes into account the stiffness of the deformable plate:

8.
$$H(\lambda(t),\chi,p(x),u(x,t)) := \frac{\lambda(t)p(x)}{(1-u(x,t))^2\Big(1+\chi\int_\Omega \frac{\mathrm{dx}}{(1-u(x,t))}\Big)^2}, \tag{3}$$
in which χ is a positive dimensionless parameter which takes into account the non-local dependence of the applied voltage, V, on the solution due to a possible non-uniform electric charge distribution; moreover, $p(x)$ is a bounded real function which takes into account the dielectric properties of the material constituting the deformable plate (as it is evident, it is independent on time) and, finally, $\lambda(t)$ is a positive dimensionless parameter depending on V, which represents the ratio of a reference electrostatic force to a reference elastic force (therefore, it depends on time).

To make (1) more adherent to industrial realities, in this work, we introduce an additive term, which, according to Pelesko and Driscoll [53–55] theory, takes the form:
$$\lambda(t)\delta(x,t)|\nabla u(x,t)|^2 \tag{4}$$
where $\delta(x,t)$ is a non-negative real function that weighs the effects due to the fringing field, so that, in our work, we replace (3) by
$$\tilde{H}(\lambda(t),\chi,\delta(x,t),p(x),u(x,t)) := \frac{\lambda(t)p(x)}{(1-u(x,t))^2\Big(1+\chi\int_\Omega \frac{\mathrm{dx}}{(1-u(x,t))}\Big)^2} + \lambda(t)\delta(x,t)|\nabla u(x,t)|^2, \tag{5}$$
and our model (1) becomes
$$\begin{cases} \Delta^2 u + c(x,t)u'(x,t) + u''(x,t) = G(\beta,\gamma,u(x,t)) + \tilde{H}(\lambda(t),\chi,\delta(x,t),p(x),u(x,t)) = \\ G(\beta,\gamma,u) + \frac{\lambda(t)p(x)}{(1-u(x,t))^2\Big(1+\chi\int_\Omega \frac{\mathrm{dx}}{(1-u(x,t))}\Big)^2} + \lambda(t)\delta(x,t)|\nabla u(x,t)|^2, \quad \text{in } \Omega\times[0,T) \\ 0 \le u(x,t) < 1, \quad \text{in } \Omega\times[0,T] \quad x\in\Omega\subset\mathbb{R}^N, \quad 1\le N<4 \\ u(x,t) = 0, \quad x\in\partial\Omega, \\ \nabla u(x,t) = 0 \quad x\in\partial\Omega. \end{cases} \tag{6}$$

We observe that in [52], system (1) was studied with Steklov boundary conditions,
$$u(x,t) = 0, \quad \nabla u(x,t) - d\frac{\partial u(x,t)}{\partial \nu} = 0, \quad \text{on } \partial\Omega\times[0,T], \tag{7}$$
in which non-negative parameter d, in the case $d=0$, gives Navier's conditions [52,56,57], in the case $d=\infty$ gives the Dirichlet's conditions $u = u_\nu = 0$; in this last case, we study our problem. To our knowledge, there are no scientific papers in the literature concerning the existence and regularity of the solution for the problem (6). Thus, in this paper, we prove these important results, which also open up interesting scenarios for possible numerical reconstructions of the deformable plate profile in the absence of ghost solutions (i.e., numerical solutions not satisfying the aforementioned conditions of existence and uniqueness).

The paper is structured as follows: After having described the studied device, specifying as the analytical model is achieved taking into account both the effect due to the fringing field and usual load conditions (Section 2), Section 3 details some peculiar properties of

the proposed model. Section 4 illustrates the main results of existence, uniqueness and regularity of the solution for (1), also providing some links with industrial specifications. In Section 5, our results concerning existence and uniqueness for (1) are proved also exploiting a penalization approach according to Campanto's Theory [58] to then proving the results of regularity in Section 6. Finally, the brief Section 7 illustrates the possible intended use of the device studied, and some conclusions and perspectives end the work.

2. Some Specifications on the Electrostatic MEMS Device and Its Analytical Model with Fringing Field

The MEMS device studied in this paper can be schematized as an elastic system consisting of two parallel plates of the same thickness and made of the same material. The upper plate, subjected to a positive electric potential, is not deformable, while the lower plate, deformable but anchored to its edges, is subjected to a reference electric potential [3]. Under the action of external V, the deformable plate lifts towards the fixed plate without touching it in order to avoid unwanted electrostatic discharges. Figure 1 displays a simplified representation of the device in which all its constituent elements are indicated.

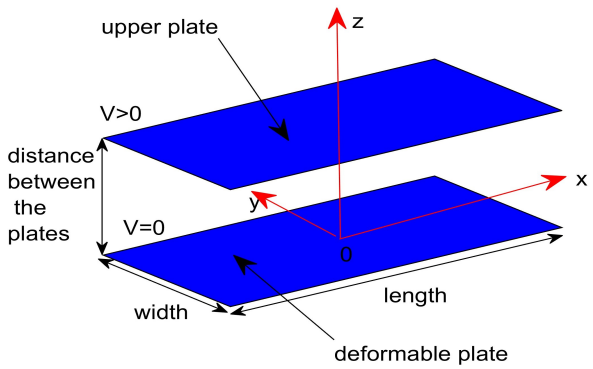

Figure 1. The electrostatic MEMS: a schematic representation.

It follows that the electrostatic potential, ϕ, satisfies, within the device, the Laplace equation, $\Delta\phi = 0$. According to the theory of deformable plates, the lower plate of the device satisfies the following equation [1,55]:

$$\tilde{K}_1(x,t)\Delta^2 u(x,t) = \tilde{K}_2(x,t)\Delta u(x,t) + \tilde{F}(x,t), \tag{8}$$

where $\tilde{K}_1(x,t)$ and $\tilde{K}_2(x,t)$ represent particular weight functions below specified and $\tilde{F}(x,t)$, defined as [1,55]

$$\tilde{F}(x,t) = \frac{\lambda(t)p(x)}{(1-u(x,t))^2}, \tag{9}$$

with

$$\lambda(t) = \frac{\epsilon_0 V^2 L^2}{2d^3 T(t)}, \tag{10}$$

(where $T(t)$ is the dynamic mechanical tension of the deformable plate, ϵ_0 is the permittivity of the free space, L is the length of the device and d is the distance between the plates) establishing how the deformable plate is stressed if V is applied. Obviously, V inside the device determines **E**, which, locally, determines an electrostatic force, which, per surface unit, materializes in electrostatic pressure acting on the deformable plate. Then, $\tilde{F}(x,t)$ must necessarily be correlated both to V (so that the deformation of the plate is controllable by V) and to the geometric, mechanical and dielectric properties of the deformable element. Therefore, combining (8) with (9), it is easy to write

$$\tilde{K}_1(x,t)\Delta^2 u(x,t) = \tilde{K}_2(x,t)\Delta u(x,t) + \frac{\lambda(t)p(x)}{(1-u(x,t))^2}, \tag{11}$$

which unfortunately is unable to electrically control the device. This is due to the fact that V must undergo a specific control action to avoid sudden lifting of the deformable plate. Then, for this purpose, it is sufficient for a basic capacitive control device consisting of an electrical circuit whose elements, connected in series with each other, are the source voltage, V_s, the capacity, C_f, of a suitable capacitor and the MEMS device to be controlled (for detail, see [1,3]). Then, as classical circuit theory suggests, the following equation holds:

$$V = \frac{V_s}{1 + \frac{C}{C_f}}, \tag{12}$$

in which C that represents the capacitance of the MEMS device; it can be easily evaluated as:

$$C = \frac{\epsilon_0}{V} \int_\Omega \nabla\phi \cdot \hat{n} \mathrm{dx} \approx \frac{\epsilon_0}{V} \int_\Omega \frac{\partial \phi}{\partial z} \mathrm{dx} \approx \frac{\epsilon_0 L^2}{d} \int_\Omega \frac{\mathrm{dx}}{(1 - u(x,t))}, \tag{13}$$

by which, setting

$$\chi = \frac{\epsilon_0 L^2}{C_f d}, \tag{14}$$

Equation (12) becomes

$$V = \frac{V_s}{1 + \chi \int_\Omega \frac{\mathrm{dx}}{(1-u(x))}}, \tag{15}$$

so that the control action on the load becomes

$$\left(\frac{V}{V_s}\right)^2 = \frac{1}{\left(1 + \chi \int_\Omega \frac{\mathrm{dx}}{(1-u(x,t))}\right)^2}. \tag{16}$$

Thus, exploiting (16), Equation (9) can be written as:

$$\tilde{F}(x) = \frac{\lambda(t)p(x)}{(1-u(x,t))^2}\left(\frac{V}{V_s}\right)^2 = \frac{\lambda(t)p(x)}{(1-u(x,t))^2\left(1 + \chi \int_\Omega \frac{\mathrm{dx}}{(1-u(x,t))}\right)^2}. \tag{17}$$

Moreover, Equation (8), by (17), becomes:

$$\tilde{K}_1(x,t)\Delta^2 u(x,t) = \tilde{K}_2(x,t)\Delta u(x,t) + \frac{\lambda(t)p(x)}{(1-u(x,t))^2\left(1 + \chi \int_\Omega \frac{\mathrm{dx}}{(1-u(x,t))}\right)^2}. \tag{18}$$

Some clarifications are necessary. In particular,

- As highlighted in Equation (14), χ essentially depends on the capacity of the device and is a positive real number less than 1 [1]. This is due to the fact that, if $\chi \to 1^-$, dangerous bifurcation phenomena capable of generating instability could occur;
- $\Delta u(x,t)$, according to the plate theory [1], takes into account the contributions due to bending and torsional curvatures;
- Since the edges of the deformable plate are anchored, once V is applied, the deformable plate rises with an evident increase in its surface (generating a "stretching effect"). Consequently, if the plate is under elastic deformation, the mechanical restoring force will necessarily be proportional to the aforementioned surface increase. The first addend of the right side of (18) contains the function $\tilde{K}_2(x,t)$ that can be expressed as

$$\tilde{K}_2(x,t) = \beta \int_\Omega |\nabla u(x,t)|^2 \mathrm{dx} + \gamma, \tag{19}$$

in which β according to Pelesko's approach [1], takes into account the stiffness of the deformable plate, and γ considers the effect due to the stretching phenomenon. Therefore,

the right side of the equation in (1), considering that, usually, $\tilde{K}_1(x,t) = \frac{D}{L^2T} \approx 1$ (where D is the flexural rigidity of the deformable plate) [1], and introducing $c(x,t)u'(x,t)$ and $u''(x,t)$ to take into account the fact that the profile of the deformable plate evolves in time, the model studied in the past was

$$\begin{cases} \Delta^2 u(x,t) + c(x,t)u'(x,t) + u''(x,t) = \\ \left(\beta \int_\Omega |\nabla u(x,t)|^2 \mathrm{dx} + \gamma\right)\Delta u(x,t) + \dfrac{\lambda(t)p(x)}{(1-u(x,t))^2\left(1+\chi \int_\Omega \frac{\mathrm{dx}}{(1-u(x,t))}\right)^2}, \\ u(x) = 0, \quad \nabla u(x) = 0, \quad x \in \partial\Omega, \\ 0 \le u(x,t) < 1, \quad \text{in } \Omega \times [0,T], \quad x \in \Omega \subset \mathbb{R}^N, \quad 1 \le N < 4. \end{cases} \tag{20}$$

We note that, in the recent past, many authors have extensively studied model (20), obtaining interesting conditions on global existence where dangerous bifurcation phenomena took place [1,59]. Particularly, in [60], it was proved that (20), besides admitting a N-dimensional generalization, provided interesting conditions of existence particularly useful for the numerical recovering of the deformable plate profile.

The Contribution Due to the Effects of the Fringing Field According to Pelesko and Driscoll Approach

We observe that, in (20), there is no contribution due to the fringing field, electrostatic phenomenon, according to which, once V is applied, the bending of **E** occurs at the edges of the MEMS, while, at its center, **E** remains parallel. Furthermore, the electrostatic capacity of the MEMS undergoes strong variations in its amplitude that are not easy to evaluate; therefore, empirical formulation has to be exploited [1,59]. As experimentally highlighted, electrostatic MEMS devices, depending on the L/d ratio, exhibit the phenomenon of the fringing field. Recently, interesting results have been obtained regarding the physico-mathematical models of parallel plate electrostatic MEMS where the effects due to the fringing field are taken into account. However, these studies are limited, for the most part, to models describing static behaviors [10,46], leaving out the evaluation of any dynamic contributions to empirical experiences. According to the Pelesko and Driscoll approach, the effects due to the fringing field are quantifiable by the following additive term [55]

$$\lambda(t)F\Big(u(x,t), \nabla u(x,t), \delta(x,t)\Big), \tag{21}$$

in which

$$F\Big(u(x,t), \nabla u(x,t), \delta(x,t)\Big) = \delta(x,t)|\nabla u(x,t)|^2 \tag{22}$$

depends on $\delta(x,t)$, which weighs the effects of this particular field; the function $\lambda(t)$, linked to V by (10), must not exceed the value of λ^* (pull-in voltage) because it would not be an essential condition for the uniqueness of the solution. This is experimentally confirmed by the fact that high values of V produce instability of the deformed plate, necessitating the enactment of control actions on V.

3. Some Properties of the Model with Fringing Field

Equation (20) takes into account many physical phenomena occurring in electrostatic MEMS with parallel plates. In the following items, some issues are detailed:

- Model (20) considers the effects due to the fringing field using a term,

$$\lambda(t)\delta(x,t)|\nabla u(x,t)|^2, \tag{23}$$

and it is easy to implement both hardware and software with obvious control by V ($\lambda \propto V$). Furthermore, the control action due to V (see (10)) allows for avoiding instabilities generating unwanted electrostatic discharges. Therefore, the intended use of the device (i.e., biomedical applications) will guarantee values of V generating stable

displacements of the deformable plate. It is worth noting that $\delta(x,t)$ cannot actually be controlled by V (as proved in literature, the deformable element is a membrane).

- The proposed model, through the β and γ, takes into account the fatigue phenomena that can arise on the deformable plate following prolonged use of the device;
- The amplitude of the variation of the electrostatic capacitance of the device, during the deformation of the plate, depends on the geometry of the device as well as on the (additional) C_f capacitance, opposing significant variations of V. The term containing χ in the proposed model takes this phenomenon into account;
- $p(x)$ in the model, which takes into account the dielectric properties of the plates, appears in the capacitive term where these properties have the greatest influence. Moreover, $p(x) \in L^2(\Omega)$ because $p(x)$ must be a measurable function so that $\forall x \in \Omega$, $|f(x)| \leq S$ (S, suitable constant).

However, it is evident that the proposed model does not allow for recovering $u(x,t)$ explicitly. Thus, for any numerical recovering, it is imperative to have conditions that ensure the existence, uniqueness and regularity of the analytical solution, which, if verified by the numerical solutions, the recovering obtained does not represent a ghost solution.

4. The Dynamic Model with Contribution Due to Fringing Field: Main Results

In [52], important existence and regularity results were proved for the (20) model, where the contribution due to the fringing field had not been considered. Particularly, for the achievement of these results, is an important theorem proved by Tarsia in [61] concerning the Near Operator Theory introduced by Campanato [58]. In the present work, exploiting the same demonstration technique, we present our main results whose proofs are detailed in Sections 5.1 and 6, respectively.

Theorem 1. *Let us consider $\Omega \subset \mathbb{R}^N$, with $1 \leq N \leq 3$, which represents a bounded domain with a sufficiently small diameter. We consider the problem (6) in which β, λ and χ are non-negative constants and both $p(x)$ and $c(x,t)$ are bounded functions while*

$$\lambda(t) \in L^{\infty}(0,T); \quad p(x) \in L^2(\Omega), \tag{24}$$

with

$$||\lambda(t)||_{\infty} < \lambda^*, \tag{25}$$

and

$$\delta(x,t) \in C^1((0,T);\ L^2(\Omega)). \tag{26}$$

Moreover, let $u_0 \in H^2 \cap H_0^1(\Omega)$ (satisfying suitable compatibility conditions) and $u_1 \in L^2(\Omega)$. Therefore, Equation (6) has a unique solution

$$u(x,t) \in C^0([0,T];\ H_0^2(\Omega)) \cap C^1([0,T];\ L^2(\Omega)). \tag{27}$$

Concerning the second-order boundary condition involved in both (1) and (6), see Remark 4, page 7 of [52].

Theorem 2. *Let us consider*

$$u(x,t) \in C^0([0,T];\ H_0^2(\Omega)) \cap C^1([0,T];\ L^2(\Omega)), \tag{28}$$

to be the solution to (6) given by Theorem 1. Assuming that

$$u_0,\ u_1 \in H^2 \cap H_0^1(\Omega), \tag{29}$$

$$\lambda(t) \in W^{1,2}(0,T), \tag{30}$$

and

$$c(x,t) \in W^{1,\infty}((0,T);\ L^2(\Omega)), \tag{31}$$

the solution enjoys the following regularity property:

$$u(x,t) \in C^0([0,T];H^4(\Omega)) \cap C^1([0,T];H^2 \cap H_0^1(\Omega)) \cap C^2([0,T];L^2(\Omega)). \tag{32}$$

Remark 1. *In Theorem 1, condition (24), as well as being mathematically necessary to prove the existence and uniqueness of the solution for (20), confirms the fact that $\lambda(t)$ must not undergo sudden variations in its amplitude. Operationally, in order for this condition to be satisfied in the experimentation, the MEMS device is associated with an electrical circuit capable of opposing the abrupt variations of V and, therefore, by the (10), there is an abrupt variation of $\lambda(t)$ (for details, see Section 2). Furthermore, to avoid bifurcation phenomena (that would contradict the uniqueness of the solution), as experimentally proved and mathematically demonstrated [1], Equation (25) must occur. This is experimentally confirmed by the fact that high values of V produce instability of the deformed plate, imposing control actions on V. Moreover, condition (24) allows us to state that*

$$\lambda(t) \in C^0(0,T). \tag{33}$$

Then, continuous waveforms for V are allowed, such as the trapezoidal ones, which, as is known, also incorporate the piecewise continuous waveforms characterized by a linear transition with a high slope between two constant levels. Finally, being

$$W^{1,2}(0,T) \subset C^0(0,T), \tag{34}$$

Equation (33) is still valid.

Remark 2. *The second-order boundary condition involved in both (1) and (6) needs to be legitimated, since, in $H^2 \cap H_0^1$, second order derivatives do not have trace on $\partial\Omega$. However, exploiting the elliptic regularity theory, the weak solution of the following problem*

$$\begin{cases} \Delta^2 u = f, & in \ \ \Omega \\ u = 0, \quad u_\nu = g, & on \ \ \partial\Omega \end{cases} \tag{35}$$

belongs to $H^4(\Omega)$, in order that $f, g \in L^2(\Omega)$. This remark allows us to rewrite the equation of our model as follows:

$$\begin{gathered} \Delta^2 u(x,t) = -c(x,t)u'(x,t) - u''(x,t) + \\ G(\beta,\gamma,u(x,t)) + \tilde{H}(\lambda(t),\chi,\delta(x,t),p(x),u(x,t)). \end{gathered} \tag{36}$$

Therefore, $\forall t \in [0,T]$, and the trace of $\Delta u(x,t)$ is well-defined on $\partial\Omega$, if the right side in (36) belongs to $L^2(\Omega)$. This condition is ensured by the regularity Theorem 5 in [52].

5. A Penalization Approach According to Campanato's Theory: The Problem of Existence and Uniqueness

To obtain the existence and uniqueness result of this paper, we use the result we achieved in the stationary case [3], and we apply opportunely the following theorem proved by Tarsia [52].

Theorem 3 ([61], Theorem 2.1)**.** *Let X be a topological space, Y a set (not necessary structured), and Z a Banach space. Let us also consider the mappings*

$$\mathbf{F} : X \times Y \to Z, \tag{37}$$

and

$$\mathbf{B} : Y \to Z. \tag{38}$$

Let us consider the following assumptions:

(i) There exists $(\mathbf{x}_0, y_0) \in X \times Y$ such that $\mathbf{F}(\mathbf{x}_0, y_0) = 0$;
(ii) The mapping $\mathbf{x} \mapsto \mathbf{F}(\mathbf{x}, y_0)$ is continuous on $\mathbf{x}_0$;

(iii) *There exists two constants, $k_1 > 0$ and $k_2 \in (0,1)$, and a neighborhood of $\mathbf{x}_0$, indicated by $U(\mathbf{x}_0) \subset X$, such that $\forall y_1, y_2 \in Y$ and $\forall \mathbf{x} \in U(\mathbf{x}_0)$, we achieve*

$$||\mathbf{B}(y_1) - \mathbf{B}(y_2) - k_1[\mathbf{F}(\mathbf{x}, y_1) - \mathbf{F}(\mathbf{x}, y_2)]||_Z \leq k_2||\mathbf{B}(y_1) - \mathbf{B}(y_2)||_Z; \tag{39}$$

(iv) $\mathbf{B}$ *is injective;*
(v) $\mathbf{B}(Y)$ *is a neighborhood of* $z_0 = \mathbf{B}(y_0)$.

Therefore, there exists a ball $S(z_0, r) \subset \mathbf{B}(Y)$ *and a neighborhood of* $\mathbf{x}_0$, *indicated by* $V(\mathbf{x}_0) \subset U(\mathbf{x}_0)$, *such that*

$$\begin{cases} \mathbf{F}(\mathbf{x}, y(\mathbf{x})) = 0, \quad \forall \mathbf{x} \in V(\mathbf{x}_0), \\ y(\mathbf{x}_0) = y_0 \end{cases} \tag{40}$$

has a unique solution

$$y : V(\mathbf{x}_0) \to \mathbf{B}^{-1}(S(z_0, r)). \tag{41}$$

Furthermore, if (iii) holds $\forall \mathbf{x} \in X$, *then the solution* $y = y(\mathbf{x})$ *turns out to be defined in the whole* X.

We apply Theorem 3 setting

$$X = \mathbb{R}^+ \times \mathbb{R}^+ \times \mathbb{R}^+ \times \Phi \times \Lambda \times \mathbb{R}^+, \tag{42}$$

in which

$$\Phi = \{f \in L^\infty(\Omega) \ : \ |x \ : \ f(x) > 0| \neq 0\}, \tag{43}$$

and

$$\Lambda = \{\lambda \in L^\infty[0,T] \ : \ 0 < \lambda < \lambda^*, \ \ \lambda^* \in \mathbb{R}^+\}. \tag{44}$$

It will be useful to prove that all assumptions of Theorem 3 are verified, and we will verify the assumptions of the Theorem 3 in order to apply it to the following penalized problem: et $\epsilon > 0$ and consider the following penalized problem

$$\begin{cases} \Delta^2 u_\epsilon(x,t) + c(x,t)u'_\epsilon(x,t) + \\ u''_\epsilon(x,t) = G(\beta, \gamma, u_\epsilon) + \tilde{H}_\epsilon(\lambda(t), \chi, p(x), \delta(x,t), u_\epsilon(x,t)), \quad \text{in } \ \Omega \times [0,T] \\ 0 < u_\epsilon(x,t) < 1, \quad \text{in } \ \Omega \times [0,T], \\ u_\epsilon(x,t) = \epsilon, \quad \text{on } \ \partial\Omega \times [0,T], \\ \Delta u_\epsilon(x,t) = 0, \quad \text{on } \ \partial\Omega \times [0,T], \\ u_\epsilon(x,0) = u_0 + \epsilon, \quad \text{on } \ \Omega, \\ u'_\epsilon(x,0) = 0, \quad \text{on } \ \Omega, \end{cases}$$

in which

$$\tilde{H}_\epsilon(\lambda(t), \chi, \delta(x,t), p(x), u(x,t)) := \\ \frac{\lambda(t)p(x)}{(1+\epsilon-u(x,t))^2\left(1+\chi\int_\Omega \frac{\mathrm{dx}}{(1-u(x,t))}\right)^2} + \lambda(t)\delta(x,t)|\nabla u(x,t)|^2. \tag{45}$$

It is worth noting that, in (45), we use $\delta(x,t)$ also for the penalized problem because, for very small variations of the profile of the deformable plate, the variation of the effects due to the fringing field is negligible. From problem (45), the following Lemma was yielded.

Lemma 1. *Let $\epsilon_0 = \sup_\Omega v_\epsilon$, where v_ϵ is the solution to the stationary problem. Under the assumption of Theorem 1, $\forall \epsilon \in \left(0, \frac{1-\epsilon_0}{2}\right)$, problem (45) admits a unique solution $u_\epsilon \in C^0([0,T]; H^2(\Omega)) \cap C^1([0,T]; L^2(\Omega))$.*

Let us define Y_ϵ as the set of functions $y \in C^0([0,T]; \mathrm{H}^2_{0,\epsilon}(\Omega)) \cap C^1([0,T]; L^2(\Omega))$, in which $\mathrm{H}^2_{0,\epsilon}(\Omega)$ indicates the set of function y such that, $\forall t \in [0,T]$, $y - \epsilon \in \mathrm{H}^2_0(\Omega))$, and

$$\Delta^2 y(x,t) + c(x,t)y'(x,t) + y''(x,t) \in L^1((0,T); L^2(\Omega)), \tag{46}$$

$$0 < y(x,t) < 1, \quad \text{in } \overline{\Omega} \times [0,T], \quad y'(x,0) = 0 \quad \text{in } \Omega, \tag{47}$$

$$\int_\Omega \frac{1}{[1-y(x,t)]^4} dx < M_1, \tag{48}$$

$$\int_\Omega |\Delta y(x,t)|^2 dx < M_2, \quad \forall t \in [0,T], \tag{49}$$

$$\int_\Omega |\nabla y(x,t)|^4 dx < M_3, \quad \forall t \in [0,T], \tag{50}$$

where M_1, M_2 and M_3 are positive constants; we also set $Z = L^1((0,T); L^2(\Omega)) \times \mathrm{H}^2_{0,\epsilon}(\Omega)$ setting

$$\mathbf{x} = (\beta, \gamma, \chi, p, \lambda, \delta), \tag{51}$$

to denote an element of the space X.

Definition 1. *Let us define*

$$\begin{aligned} \mathbf{F}_\epsilon(\mathbf{x}, y) := (F_\epsilon(x,y), y(x,0), y'(x,0)) = \\ (\Delta^2 y(x,t) + c(x,t)y'(x,t) + y''(x,t) - \\ -G(\beta, \gamma, y(x,t)) - \tilde{H}(\lambda(t), \chi, p(x), y(x,t), \delta(x,t), y(x,t)), \\ (y(x,0) - \epsilon - u_0)|\lambda(t) - \lambda_0|), \end{aligned} \tag{52}$$

$$\begin{aligned} \mathbf{B}(y) := (B(y), y(x,0)) = \\ (\Delta^2 y(x,t) + c(x,t)y'(x,t) + y''(x,t)y(x,0)). \end{aligned} \tag{53}$$

We remark that the existence of the solution v_ϵ of the stationary problem obtained by (45), for a fixed t, follows from the existence of the solution v_0 corresponding to $\epsilon = 0$ achieved in [3], by considering $0 < \epsilon < (1-\epsilon_0)/2$ and setting $v_\epsilon = v_0 + \epsilon$.

5.1. Proofs of Theorem 1 and Lemma 1

Now, we prove Theorem 1 and Lemma 1 applying Theorem 3 and, for this purpose, we will prove that the assumptions $(i) - (v)$ are verified for the penalized problem (45). Thus, we set

$$\mathbf{x}_0 = (\beta_0, \gamma_0, \chi_0, p_0, \lambda_0, \delta_0) \quad \text{and} \quad y_{0,\epsilon} = v_\epsilon(x, t_0), \tag{54}$$

to obtain

$$\mathbf{F}_\epsilon(\mathbf{x}_0, y_{0,\epsilon}) = 0. \tag{55}$$

To verify (ii), we have to evaluate

$$\begin{aligned}
&||\mathbf{F}_\epsilon(\mathbf{x}, y_{0,\epsilon}) - \mathbf{F}_\epsilon(\mathbf{x}_0, y_{0,\epsilon})||_Z = \\
&\int_0^T \int_\Omega |F_\epsilon(\beta, \gamma, \chi, p(x), \lambda(t), \delta(x,t), v_\epsilon(x,t_0)) - \\
&F_\epsilon(\beta_0, \gamma, \chi_0, p_0(x), \lambda_0(t), \delta_0, v_\epsilon(x,t_0))|^2 dxdt \leq \\
&2\int_0^T \int_\Omega \Big| \Big[\beta \int_\Omega |\nabla v_\epsilon(x,t_0)|^2 dx + \gamma\Big] \Delta v_\epsilon(x,t_0) - \\
&\Big[\beta_0 \int_\Omega |\nabla v_\epsilon(x,t_0)|^2 dx + \gamma_0\Big] \Delta v_\epsilon(x,t_0)\Big|^2 dxdt + \\
&2\int_0^T \int_\Omega \Big| \frac{\lambda(t)p(x)}{[1+\epsilon v_\epsilon(x,t_0)]^2[1+\chi h(v_\epsilon)]^2} - \\
&\frac{\lambda_0(t)p_0(x)}{[1+\epsilon - v_\epsilon(x,t_0)]^2[1+\chi_0 h(v_\epsilon)]^2}\Big|^2 dxdt + \\
&2\int_0^T \int_\Omega \Big|\lambda(t)\delta(x,t)|\nabla v_\epsilon(x,t_0)|^2 - \lambda_0\delta(x,t_0)|\nabla v_\epsilon(x,t_0)|^2\Big|^2 dxdt = I_1 + I_2 + I_3.
\end{aligned} \tag{56}$$

For this purpose, exploiting what has been demonstrated in this regard in [52], there remains to study the term due to the fringing field that is to increase I_3, that is, exploiting the Sobolev embedding theorem (because $N < 4$)

$$\begin{aligned}
I_3 = 2\int_0^T \int_\Omega \Big|\lambda(t)\delta(x,t)|\nabla v_\epsilon(x,t_0)|^2 - \lambda_0\delta_0\nabla v_\epsilon(x,t_0)|^2\Big|^2 dxdt \leq \\
||\lambda - \lambda_0||_{L^\infty(0,T)}||\delta - \delta_0||_{L^\infty((0,T);\Omega)} T||\nabla_\epsilon(x,t_0)||^4_{L^4(\Omega)} \leq \\
C(T,\Omega,M_3)||\lambda - \lambda_0||_{L^\infty(0,T)}||\delta - \delta_0||_{L^\infty((0,T);\Omega)}
\end{aligned} \tag{57}$$

where $\delta_0 = \delta(x,t_0)$. As consequence of [3], we have proved that, for any $(\beta_0, \gamma_0, \chi_0, p_0) \in \mathbb{R}^+ \times \mathbb{R}^+ \times \mathbb{R}^+ \times \Phi \times \mathbb{R}^+$, and $\forall t_0 \in [0,T]$ and $\lambda_0 \in [0, \lambda^*)$, there exists a unique stationary solution, $v_\epsilon(x,t_0) \in \mathrm{H}^2_0(\Omega) \cap \mathrm{H}^4(\Omega)$ of the problem achieved from (45) by freezing the time at $t = t_0$, which satisfies $0 < v_\epsilon(x,t_0) < 1$ together with

$$\int_\Omega \frac{1}{[1 - v_\epsilon(x,t_0)]^2} dx < M_1, \tag{58}$$

$$\int_\Omega |\Delta v_\epsilon(x,t_0)|^2 dx < M_2, \tag{59}$$

$$\int_\Omega |\nabla v_\epsilon(x,t_0)|^4 dx < M_3, \tag{60}$$

provided the diameter of Ω is sufficiently small.

In order to prove estimate (iii) of Theorem 3 in the global form holds, we need to prove that there exists $k_1 > 0$ and $k_2 \in (0,1)$ such that $\forall \mathbf{x} \in X, y_1, y_2 \in Y_\epsilon$, the following inequality is yielded:

$$\begin{aligned}
&\int_0^T \int_\Omega |(1-k_1)[B(y_1) - B(y_2)] + \\
&k_1|G(\beta,\gamma,y_1(x,t)) - \tilde{H}_\epsilon(\lambda(t),\chi,p(x),y_1(x,t),\delta(x,t),y_1(x,t))] - \\
&[G(\beta,\gamma,y_2(x,t)) - \tilde{H}_\epsilon(\lambda(t),\chi,p(x),y_2(x,t),\delta(x,t),y_2(x,t))]|^2 dxdt + \\
&(1-k_1)^2||\lambda(t) - \lambda||^2_{\infty,[0,T]}||y_1(x,0) - y_2(x,0)||^2_{\mathrm{H}^2_0(\Omega)} \leq \\
&k_2\int_0^T \int_\Omega |\Delta^2 y_1(x,t) + c(x,t)y_1'(x,t) + y_1''(x,t) - \\
&[\Delta^2 y_2(x,t) + c(x,t)y_2'(x,t) + y_2''(x,t)]|^2 dxdt + k_2||y_1(x,0) - y_2(x,0)||^2_{\mathrm{H}^2_0(\Omega)}.
\end{aligned} \tag{61}$$

After observing that the initial data comply with (61), provided we chose $(1-k_1) \leq k_2$, the next step concerns the evaluation of the integral part and then we begin to estimate

$$\int_0^T \int_\Omega |G(\beta,\gamma,y_1(x,t)) - G(\beta,\gamma,y_2(x,t))|^2 dxdt. \tag{62}$$

For this purpose, we exploit the calculation as in [52] achieving the following:

$$\begin{aligned} &\int_0^T \int_\Omega |G(\beta,\gamma,y_1(x,t)) - G(\beta,\gamma,y_2(x,t))|^2 dxdt \leq \\ &C(\beta,\gamma,M_2,d_\Omega) e^{2T||c||_\infty} \Big\{ [\int_0^T \Big(\int_\Omega |B(y_1) - B(y_2)|^2 dx \Big)^{\frac{1}{2}} dt]^2 + \\ &\qquad ||y_1(x,0) - y_2(x,0)||^2_{\mathrm{H}_0^2(\Omega)} \Big\}. \end{aligned} \tag{63}$$

Arguing as in [52], to complete the proof, we need to increase

$$\int_0^T \int_\Omega |\tilde{H}_\epsilon(\lambda(t),\chi,\delta(x,t),p(x),u_\epsilon) - \tilde{H}_{\epsilon_1}(\lambda(t),\chi,\delta(x,t),p(x),u_{\epsilon_1})|^2 dxdt. \tag{64}$$

Therefore,

$$\begin{aligned} &\int_0^T \int_\Omega |\tilde{H}_\epsilon(\lambda(t),\chi,p(x),y_1(x,t),\delta(x,t),y_1(x,t)) - \\ &\tilde{H}_\epsilon(\lambda(t),\chi,p(x),y_2(x,t),\delta(x,t),y_2(x,t))|^2 dxdt = \\ &\int_0^T \int_\Omega \Big| \frac{\lambda(t)p(x)}{[1+\epsilon-y_1(x,t)]^2[1+\chi h(y_1)]^2} + \lambda(t)\delta(x,t)|\nabla y_1(x,t)|^2 - \\ &\frac{\lambda(t)p(x)}{[1+\epsilon-y_2(x,t)]^2[1+\chi h(y_2)]^2} - \lambda(t)\delta(x,t)|\nabla y_2(x,t)|^2 \Big|^2 dxdt \leq \\ &2(\lambda^*)^2 ||p||^2_{L^\infty(\Omega)} \int_0^T \int_\Omega \Big| \frac{(1+\epsilon-y_2(x,t))^2 - (1+\epsilon-y_1(x,t))^2}{(1+\epsilon-y_2(x,t))^2(1+\epsilon-y_1(x,t))^2} \Big|^2 + \\ &\Big| \frac{[1+\chi h(y_2)]^2 - [1+\chi h(y_1)]^2}{(1+\epsilon-y_2(x,t))^2} \Big|^2 dxdt + \\ &\int_0^T \int_\Omega (\lambda(t)\delta(x,t)) \Big| |\nabla y_1(x,t)|^2 - \lambda(t)\delta(x,t)(|\nabla y_2(x,t)|^2) \Big|^2 dxdt = \\ &2(\lambda^*)^2 ||p||^2_{L^\infty(\Omega)} (IH_1 + IH_2) + IH_3. \end{aligned} \tag{65}$$

Both IH_1 and IH_2 have been elaborated in [52] achieving the following inequalities:

$$\begin{aligned} IH_1 \leq 4CM_1^2 T d_\Omega^{4-N} e^{2T||c||_\infty} \Big\{ \Big[\int_0^T \Big(\int_\Omega |B(y_1) - B(y_2)|^2 dx \Big)^{\frac{1}{2}} dt \Big]^2 + \\ + ||y_1(x,0) - y_2(x,0)||^2_{\mathrm{H}_0^2(\Omega)} \Big\}, \end{aligned} \tag{66}$$

$$\begin{aligned} IH_2 \leq C(\chi,M_1,|\Omega|) T d_\Omega^2 e^{2T||c||_\infty} \Big\{ \Big[\int_0^T \Big(\int_\Omega |B(y_1) - B(y_2)|^2 dx \Big)^{\frac{1}{2}} dt \Big]^2 + \\ ||y_1(x,0) - y_2(x,0)||^2_{\mathrm{H}_0^2(\Omega)}. \end{aligned} \tag{67}$$

It remains to elaborate IH_3, that is,

$$\begin{aligned} IH_3 = \int_0^T \int_\Omega \Big|(\lambda(t)\delta(x,t)|\nabla y_1(x,t)|^2 - \lambda(t)\delta(x,t)(|\nabla y_2(x,t)|^2\Big|^2 dxdt \leq \\ (\lambda^*)^2||\delta||^2_{L^\infty(\Omega\times[0,T])} \int_0^T \int_\Omega \Big||\nabla y_1(x,t) + \nabla y_2(x,t)||\nabla y_1(x,t) - \nabla y_2(x,t)|\Big|^2 dxdt \leq \\ (\lambda^*)^2||\delta||^2_{L^\infty(\Omega\times[0,T])} \int_0^T \Big(\int_\Omega |\nabla(y_1(x,t) + y_2(x,t)|^4 dx\Big)^{\frac{1}{2}} \\ \Big(\int_\Omega |\nabla(y_1(x,t) - y_2(x,t)|^4 dx\Big)^{\frac{1}{2}} dt \leq \\ (\lambda^*)^2||\delta||^2_{L^\infty(\Omega\times[0,T])} C(T) \sup_{t\in[0,T]} ||\nabla(y_2(x,t) + y_2(x,t))||^2_{L^\infty(\Omega)} \\ \int_0^T ||\nabla(y_2(x,t) - y_1(x,t))||^2_{L^4(\Omega)} dt. \end{aligned} \tag{68}$$

To increase the last integral in (68), we increase

$$||\nabla(y_2(x,t) - y_2(x,t))||^2_{L^4(\Omega)}, \tag{69}$$

using Sobolev's embedding theorem, Poincaré and Miranda-Talenti inequalities and, in particular,

$$\int_\Omega |\nabla y_1(x,t)|^2 dx \leq C d_\Omega^2 \int_\Omega |\Delta y_1(x,t)|^2 dx. \tag{70}$$

Then, by Gronwall's Lemma, we have

$$\begin{aligned} IH_3 \leq C(M_2, d_\Omega, \delta) e^{2T||c||_\infty} \\ \Big\{\Big[\int_0^T \Big(\int_\Omega |B(y_1) - B(y_2)|^2 dx\Big)^{\frac{1}{2}} dt\Big]^2 + ||y_1(x,0) - y_2(x,0)||^2_{H_0^2}\Big\}, \end{aligned} \tag{71}$$

and then, with d_Ω being sufficiently small (this is physically correct because, usually, the amplitude of the deformation of the deformable plate has dimensions of the order of 10^{-6}), we have proved that property (iii) is verified.

To verify condition (v) in Theorem 3, we need to prove that, for $\eta > 0$, such that, $\forall g \in L^1((0,T); L^2(\Omega))$ satisfying

$$\int_0^T \int_\Omega |g - \mathbf{B}y_{0,\epsilon}|^2 dxdt < \eta^2, \tag{72}$$

we can find $u_\epsilon \in Y_\epsilon$ such that $Bu_\epsilon = g$. As already noted in [61], $y_{0,\epsilon} \in Y_\epsilon \cap H^4(\Omega)$ and $y'_{0,\epsilon} = y''_{0,\epsilon} = 0$ so that $By_{0,\epsilon} = \Delta^2 y_{0,\epsilon} \in L^2(\Omega)$. Moreover, it is known that the following Cauchy–Dirichlet problem

$$\begin{cases} Bu_\epsilon(x,t) = \Delta^2 u_\epsilon(x,t) + c(x,t)u'_\epsilon(x,t) + u''_\epsilon(x,t) = f(x,t), \quad \text{a.e. in } \Omega\times[0,T], \\ u_\epsilon(x,0) = y_{0,\epsilon}, \quad \text{in } \Omega, \\ u'_\epsilon(x,0) = 0, \quad \text{a.e. in } \Omega, \\ u_\epsilon(x,t) = \epsilon, \quad \text{in } \partial\Omega\times[0,T], \\ \Delta u_\epsilon = 0, \quad \text{in } \partial\Omega\times[0,T], \end{cases} \tag{73}$$

by means of Theorem 3 in [52], which can also be easily applied in the presence of the term due to the fringing field, has a unique solution $y_\epsilon \in C^0((0,T)\mathrm{H}^2_{0,\epsilon}) \cap C^1((0,T); L^2(\Omega))$. Now, we need to verify the remaining conditions for functions belonging to Y_ϵ. For this purpose, applying to $u_\epsilon - y_{0,\epsilon}$ the energy estimation (12) in [52] with

$$f(x,t) = G(\beta,\gamma,u(x,t)) + \tilde{H}(\lambda(t),\chi,\delta(x,t),p(x),u(x,t)), \tag{74}$$

we have that, $\forall t \in [0,T]$:

$$\int_\Omega |\Delta u_\epsilon(x,t) - \Delta y_{0,\epsilon}(x)|^2 dx \leq e^{2t||c||_\infty} \Big\{ \Big[\int_0^T \Big(\int_\Omega |B(u_\epsilon) - B(y_{0,\epsilon})|^2 dx \Big)^{\frac{1}{2}} \Big]^2 \Big\}. \tag{75}$$

Since

$$\int_\Omega |\Delta y_{0,\epsilon}(x)|^2 dx < M_2, \quad \forall t \in [0,T], \tag{76}$$

it is easy to see that

$$\int_\Omega |\Delta u_\epsilon(x,t)|^2 dx < M_2 \quad \forall t \in [0,T]. \tag{77}$$

If η is small enough, this implies condition (49). We recall that $1 \leq N < 4$, exploiting the Sobolev embedding theorem, it is easy to write

$$\sup_\Omega |u_\epsilon(x,t) - y_{0,\epsilon}| \leq C\Big(d_\Omega^{2-\frac{N}{2}}\Big) ||\Delta u_\epsilon(x,t) - y_{0,\epsilon}(x)||_{L^2(\Omega)} < C\Big(d_\Omega^{2-\frac{N}{2}}\Big)\eta. \tag{78}$$

Since $0 < y_{0,\epsilon} < 1$, $\forall x \in \overline{\Omega}$, there exists $\eta_1 > 0$ such that, for $0 < \eta < \eta_1$, also $0 < u_\epsilon(x,t) < 1$ and then condition (47) is satisfied. Then, we conclude that (v) is satisfied and, thus, all assumptions of Theorem 3 are verified. Finally, taking into account the same calculations carried out in [52], Lemma 1 is verified. In fact, from the following inequality

$$\begin{aligned} &\int_\Omega \frac{1}{(1-u_\epsilon(x,t))^2} dx \leq \\ &\int_\Omega \Big| \frac{(1-u_\epsilon)^2 - (1-y_{0,\epsilon})^2}{(1-y_{0,\epsilon})^2(1-u_\epsilon)^2} \Big| dx + \int_\Omega \frac{1}{(1-y_{0,\epsilon})^2} dx, \end{aligned} \tag{79}$$

and following the same procedure to verify condition (ii), it is very easy to achieve

$$\int_\Omega \Big| \frac{(1-u_\epsilon)^2 - (1-y_{0,\epsilon})^2}{(1-y_{0,\epsilon})^2(1-u_\epsilon)^2} \Big| dx \leq C \sup_\Omega |u - y_{0,\epsilon}|, \tag{80}$$

and, exploiting inequality (78), it follows that there exists $\eta_2 > 0$, such that, for $0 < \eta < \eta_2$, it follows that

$$\int_\Omega \frac{1}{(1-y_{0,\epsilon})^2} dx < M_1, \quad \forall t \in [0,T], \tag{81}$$

so hence condition (5) concludes the proof of Lemma 1.

Now, we show that the solution of the penalized problem, u_ϵ, converges, as $\epsilon \to 0$ to the solution of (6). For this purpose, we need to prove that the family of the penalized solution has a Cauchy sequence in $C^0([0,T]; \mathrm{H}_0^2 \cap C^1([0,T]; L^2(\Omega))$. Indeed, if u_ϵ and u_{ϵ_1} are two penalized solutions corresponding to parameters ϵ and ϵ_1, respectively, and we consider

$$\begin{cases} \Delta^2(u_\epsilon(x,t) - u_{\epsilon_1}(x,t)) + c(x,t)(u'_\epsilon(x,t) - u'_{\epsilon_1}(x,t)) + u''_\epsilon(x,t) + u''_{\epsilon_1}(x,t) + \\ G(\beta,\gamma,u_\epsilon(x,t)) - G(\beta,\gamma,u_{\epsilon_1}(x,t)) = \\ \tilde{H}_\epsilon(\lambda(t),\chi,\delta(x,t),p(x),u_\epsilon(x,t)) - \\ \tilde{H}_{\epsilon_1}(\lambda(t),\chi,\delta(x,t),p(x),u_{\epsilon_1}(x,t)), \quad \text{in } \Omega \times [0,T] \\ u_\epsilon(x,t) - u_{\epsilon_1}(x,t) = \epsilon - \epsilon_1, \\ \Delta[u_\epsilon(x,t) - u_{\epsilon_1}(x,t)] = 0, \quad \text{on } \partial\Omega \times [0,T], \\ u_\epsilon(x,0) = \epsilon - \epsilon_1, \quad \text{on } \Omega, \\ (u'_\epsilon - u'_{\epsilon_1})(x,0) = 0, \quad \text{on } \Omega, \end{cases} \tag{82}$$

arguing as in [52], and proceeding as in (68) concerning the increasing of the term related to the fringing field, we can write, $\forall t \in [0, T]$,

$$\int_0^t \int_\Omega |G(\beta, \gamma, u_\epsilon(x,t)) - G(\beta, \gamma, u_{\epsilon_1}(x,t))|^2 dxdt \leq C \int_0^t \int_\Omega |\Delta[u_\epsilon(x,t) - u_{\epsilon_1}(x,t)]|^2 dxdt, \tag{83}$$

and again

$$\int_0^t \int_\Omega |\tilde{H}_\epsilon(\lambda(t), \chi, \delta(x,t), p(x), u_\epsilon(x,t)) - \tilde{H}_{\epsilon_1}(\lambda(t), \chi, \delta(x,t), p(x), u_{\epsilon_1}(x,t))|^2 dxdt \leq \tag{84}$$

$$C(\epsilon - \epsilon_1)^2 T|\Omega| + C_2 \int_0^t \int_\Omega |\Delta[u_\epsilon(x,t) - u_{\epsilon_1}(x,t)]|^2 dxdt. \tag{85}$$

Therefore, applying inequality (12) in [52] to the model (82), $\forall t \in [0, T]$, we can write:

$$\int_\Omega |\Delta[u_\epsilon(x,t) - u_{\epsilon_1}(x,t)]|^2 dx \leq C(\epsilon - \epsilon_1)^2 T|\Omega| + C_2 \int_0^t \int_\Omega |\Delta[u_\epsilon(x,t) - u_{\epsilon_1}(x,t)]|^2 dxdt, \tag{86}$$

and, applying the Gronwall's Lemma, the following inequality yields

$$\int_\Omega |\Delta[u_\epsilon(x,t) - u_{\epsilon_1}(x,t)]|^2 dx \leq C(\epsilon - \epsilon_1)^2 T|\Omega|, \tag{87}$$

which completes the proof of Theorem 1.

Remark 3. *It is worth noting that there are MEMS devices which rely on the fact that $\lambda(t) > \lambda^*$, $\forall t$, in which the point of maximum deflection continues to advance suddenly until its movement is interrupted by contact with a dielectric that prevents the short circuit [62,63]. However, we observe that the proposed model starts from a fourth order dynamic model for a MEMS device in which the deformable element is a metal plate. In the work we propose, a term has been added to this model in order to take into account the effects due to the fringing field. Operationally, we started from the statement of Theorem 1 which sanctioned the existence and uniqueness of the solution of the starting theorem in which $\lambda(t) > \lambda^*$. However, as proof of this, in the proof of Theorem 1, it was necessary more than once to extract $\lambda(t)$ from the integrals in the time domain. This operation is feasible on the assumption that there exists a λ^* (independent of t) which increases, $\forall t$, $\lambda(t)$.*

6. A Result Concerning the Regularity (Proof of Theorem 2)

To prove the regularity of the solution for (6) (Theorem 2), we exploit the same procedure as for the proof of Theorem 2 in [52] and also utilize its Lemma 3 (obviously, adapting the procedure to our model). We premise the following result of regularity proved by Gilardi [52]).

Theorem 4. *Let V, H be Hilbert spaces such that $V \hookrightarrow H \hookrightarrow V'$ with continuous and dense embeddings. Let* **A**. **R** *and* **C** *be linear operators as defined in [52]. Let us consider the following Cauchy problem:*

$$\begin{cases} \mathbf{A}u(t) + \mathbf{R}(t)u(t) + \mathbf{C}(t)u'(t) + u''(t) = f(t), \quad t \in [0, T], \\ u(0) = u_0, \\ u'(0) = 0, \end{cases} \tag{88}$$

where $f \in L^1((0,T);H)$ *and* $u_0 \in V$. *Let* $f \in W^{1,1}((0,T);H)$, $u_0, u_1 \in V$ *and* $Au_0 \in V$. *Moreover, let* $\mathbf{R}(t)$ *and* $\mathbf{C}(t)$ *in* $W^{1,1,}(0,T)$. *Furthermore, for any* $v \in V$,

$$||\mathbf{R}'(t)v||_H \leq c||v||_V, \tag{89}$$

and, for any $v \in H$,

$$||\mathbf{C}'(t)v||_H \leq c||v||_H. \tag{90}$$

Then, the solution u *of* (88), *if* $c \in H^{1,\infty}((0,T);L^2(\Omega))$, *belongs to*

$$C^0([0,T];D(A)) \cap C^1((0,T);V) \cap C^2((0,T);H). \tag{91}$$

We recall that Equation (6) can be writable as follows:

$$\begin{aligned} \Delta^2 u(x,t) + \Big[-\beta \int_\Omega |\nabla u(x,t)|^2 dx + \gamma \Big] \Delta u(x,t) + c(x,t)u'(x,t) + u''(x,t) = \\ \tilde{H}(\lambda(t), \chi, \delta(x,t), p(x), u(x,t)) = \\ \frac{\lambda(t)p(x)}{(1-u(x,t))^2 \Big(1 + \chi \int_\Omega \frac{\mathrm{dx}}{(1-u(x,t))}\Big)^2} + \lambda(t)\delta(x,t)|\nabla u(x,t)|^2 \end{aligned} \tag{92}$$

so that, applying Theorem 1, the right-hand side of the previous equation

$$\frac{\lambda(t)p(x)}{(1-u(x,t))^2 \Big(1 + \chi \int_\Omega \frac{\mathrm{dx}}{(1-u(x,t))}\Big)^2} + \lambda(t)\delta(x,t)|\nabla u(x,t)|^2, \tag{93}$$

belongs to $C^2([0,T];L^2(\Omega)$ provided

$$\lambda(t)p(x) \in C^1([0,T];L^2(\Omega)), \tag{94}$$

so that, by Lemma 3 of [52] (this is allowed because (27) is valid),

$$t \mapsto -\beta \int_\Omega |\nabla u(x,t)|^2 dx + \gamma, \tag{95}$$

belongs to $H^{1,\infty}(0,T)$. Therefore, exploiting Theorem (4), we can write

$$u(x,t) \in C^0([0,T];H^4(\Omega)) \cap C^1([0,T];H^2 \cap H_0^1(\Omega)) \cap C^2[0,T];L^2(\Omega)), \tag{96}$$

provided

$$c \in H^{1,\infty}((0,T);L^2(\Omega)), \tag{97}$$

which concludes the proof of Theorem 2.

7. Possible Uses of the Device Studied

As per experimental evidence known in the literature, electrostatic MEMS devices with parallel plates (whose use is currently quite wide and in continuous growth) do not require particular precautions for their realization (even on an industrial scale) so the associated costs to a possible industrial production are quite contained. Furthermore, as discussed above, the fields of application are all those for which the operating voltages would be rather contained. These applications include biomedical ones, which, as is known, subject the deformable element to periodic and prolonged loads with evident risks of fatigue and breakage. While aware that circular membrane devices perform better than devices in which the deformable element is a rectangular metal plate (or membrane) (since fatigue and failure occur with very low probability), we believe that the studied device, if realized, can also be used for biomedical applications (i.e., micropumps for the intravenous administration of drugs and the high-precision surgical microsystems) as

long as it is associated with a guarantee period provided by the manufacturer compatible with the resistance of the material of the deformable plate to prolonged and continuous stresses, beyond which the device, even if still functional, must be replaced. This use is also supported by the fact that the study carried out has highlighted that continuous waveforms for V are allowed, such as the trapezoidal ones as well as piecewise continuous waveforms with a linear transition (V waveforms typical of micropumps).

8. Conclusions and Perspectives

In this paper, a new version of a dynamic hyperbolic fourth-order dimensionless integro-differential model for electrostatic MEMS devices with parallel plates for industrial and biomedical uses, taking into account, according to Pelesko & Driscoll approach, the effects due to the fringing field, has been proposed and studied. The model, controlling the behavior in external electrical voltage, considers both stiffness and self-stretching of the deformable plate, making the device suitable for any uses where limited external electrical voltages are required (i.e., continuous waveforms, trapezoidal ones incorporating piecewise continuous waveforms with high-slope linear transitions). This model does not allow the explicit recovering of the deformable profile. Therefore, by well-known results on the theory of neighboring operators, uniqueness and regularity of the solution have been proven, making possible in the future any no-ghost numerical recovery (i.e., numerical solutions that do not satisfy the conditions of existence, uniqueness and regularity). Moreover, the uniqueness of the solution ensures that each value of external tension applied determines only one deformation of the deformable plate. Furthermore, since the results are valid for $N < 4$, the model satisfies the requirement of developing 3D predictive models in which stiffness and self-stretching and fringing field effects are considered. In addition, being $N < 4$, the model is also valid for devices with thin dielectric layers (in which fringing field occurs) in which at least one spatial dimension can be neglected (the term taking these phenomena into account strongly depends on $\lambda(t)$ which strongly increases as the distance between the two plates of the device decreases). However, in the model, the parameter that weighs the effects due to the fringing field is not controllable in voltage. Therefore, efforts will be focused on defining the link between this parameter and the external voltage, to reduce the risk of triggering unwanted electrostatic discharges, even in cases where defects and/or anomalies in the deformable plate could occur. The present work, obviously, is to be considered as the first step of a broader research path where the numerical recovery of the deformable plate profile will have to be performed in the near future with numerical techniques for the resolution of integro-differential hyperbolic dynamic models (FEM, finite differences, or other). Furthermore, the existence conditions' uniqueness and regularity of the solution obtained in this work, if satisfied by any numerical solutions, will provide recoveries of the deformable plate profile that will not represent ghost solutions (i.e., numerical solutions that do not satisfy the existence, uniqueness and regularity conditions of the solution of the analytical model).

Author Contributions: Conceptualization, P.D.B., L.F. and M.V.; methodology, L.F. and M.V.; validation, P.D.B. and L.F.; formal analysis, L.F. and M.V.; investigation, P.D.B. and M.V.; resources, P.D.B., L.F. and M.V.; writing—original draft preparation, M.V.; writing—review and editing, P.D.B. and L.F.; supervision, P.D.B., L.F. and M.V. All authors have read and agreed to the published version of the manuscript.

Funding: This research received no external funding.

Institutional Review Board Statement: Not applicable.

Informed Consent Statement: Not applicable.

Conflicts of Interest: The authors declare no conflict of interest.

Abbreviations

The following abbreviations are used in this manuscript:

MEMS	micro-electro-mechanical systems
Ω	smooth bounded domain
V	external electrostatic potential
x	spatial variable
t	time
$u(x,t)$	unknown profile of the deflecting plate
χ	the dimensionless parameter that weighs the capacitance of the MEMS
$\lambda(t)$	drop-in voltage
$p(x)$	bounded real function taking into account the dielectric properties of the material
$\delta(x,t)$	the real parameter that weighs the effect of the fringing field
N	dspace dimension
ν	outward pointing normal to $\partial\Omega$
$c(x,t)$	bounded real function related to anisotropic damping phenomena
d	distance between the plates in the MEMS
L	the length of the MEMS
$\tilde{F}(x)$	load function
$T(t)$	the mechanical tension of the deformable plate at rest
ϵ_0	the permittivity of free space
V_s	source voltage
C_f	the capacitance of the fixed series capacitor
C	the capacitance of the MEMS device
D	flexural rigidity
$\tilde{K}_1(x)$, $\tilde{K}_2(x)$	specific weight functions

References

1. Ai, S.; Pelesko, J.A. Dynamics of a Canonical Electrostatic MEMS/NEMS System. *J. Dyn. Differ. Equ.* **2008**, *20*, 609–641. [CrossRef]
2. Fitzgerald, A.M.; White C.D.; Chung C.C. *MEMS Produc Development*; Springer: Cham, Switzerland, 2021.
3. Di Barba, P.; Fattorusso, L.; Versaci, M. Electrostatic-Elastic MEMS with Fringing Field: A Problem of Global Existence. *Mathematics* **2022**, *10*, 54. [CrossRef]
4. Hasan, M.H.; Abbasalipour, A.; Nikfarjam, H.; Pourkamali, S.; Emad-Ud-Din, M.; Jafari, R.; Alsaleem, F. Exploiting Pull-In/Pull-Out Hysteresis in Electrostatic MEMS Sensor Networks to Realize a Novel Sensing Continuous-Time Recurrent Neural Network. *Micromachines* **2021**, *12*, 268. [CrossRef] [PubMed]
5. Morkvenaite-Vilkonciene, I.; Bucinskas, V.; Subaciute-Zemaitiene, J.; Sutinys, E.; Virzonis, D.; Dzedzickis, A. Development of Electrostatic Microactuators: 5-Year Progress in Modeling, Design, and Applications. *Micromachines* **2022**, *13*, 1256. [CrossRef]
6. Khaled, A.; Salman, A.M.; Aljehani, N.S.; Alzahem, I.F.; Almikhlafi, R.S.; Noor, R.M.; Seddiq, Y.M.; Alghamdi, M.S.; Soliman, M.; Mahmoud, M.A.E. An Electrostatic MEMS Roll-Pitch Rotation Rate Sensor with In-Plane Drive Mode. *Sensors* **2022**, *22*, 702. [CrossRef]
7. Chung, M.; Jeong, H.; Kim, Y.-K.; Lim, S.; Baek, C.-W. Design and Fabrication of Millimeter-Wave Frequency-Tunable Metamaterial Absorber Using MEMS Cantilever Actuators. *Micromachines* **2022**, *13*, 1354. [CrossRef]
8. Xu, R.-J.; Lin, Y.-S. Actively MEMS-Based Tunable Metamaterials for Advanced and Emerging Applications. *Electronics* **2022**, *11*, 243. [CrossRef]
9. Greco, A.; Costantino, D.; Morabito, F.C.; Versaci, M. A Morlet Wavelet Classification Technique for ICA Filtered sEMG Experimental Data. In Proceedings of the International Joint Conference on Neural Networks, Portland, OR, USA, 20–24 July 2003.
10. Versaci, M.; Jannelli, A.; Morabito, F.C.; Angiulli, G. A Semi-Linear Elliptic Model for a Circular Membrane MEMS Device Considering the Effect of the Fringing Field. *Sensors* **2021**, *21*, 5237. [CrossRef]
11. Angiulli, G.; Jannelli, A.; Morabito, F.C.; Versaci, M. Reconstructing the Membrane Detection of a 1D Electrostatic-Driven MEMS Device buy the Shooting Method: Convergence Analysis and Ghost Solution Identification. *Comput. Appl. Math.* **2018**, *37*, 4484–4498. [CrossRef]
12. Tseng, S.H. CMOS MEMS Design and Fabrication Platform. *Front. Mech. Eng.* **2022**, *8*, 894484. [CrossRef]
13. Girija Sravani, K.; Rao, S. A modified proposed capacitance model for step structure capacitive RF MEMS switch by incorporating fringing field effects. *Int. J. Electron.* **2020**, *107*, 1822–1843. [CrossRef]
14. Faraci, D.; Zega, V.; Nastro, A.; Comi, C. Identification of MEMS Geometric Uncertainties through Homogenization. *Micro* **2022**, *2*, 564–574. [CrossRef]

15. Salem, M.S.; Zekry, A.; Abouelatta, M.; Shaker, A.; Salem, M.S. Validation and Evaluation of a Behavioral Circuit Model of an Enhanced Electrostatic MEMS Converter. *Micromachines* **2022**, *13*, 868. [CrossRef] [PubMed]
16. Kuru, K.; Ansell, D.; Jones, M.; Watkinson, B.J.; Caswell, N.; Leather, P.; Lancaster, A.; Sugden, P.; Briggs, E.; Davies, C.; et al. Intelligent Autonomous Treatment of Bedwetting Using Non-Invasive Wereable Advanced Mechatronics Systems and MEMS Sensors. *Med. Biol. Eng. Comput.* **2020**, *58*, 943–965. [CrossRef]
17. Podbiel, D.; Laermer, F.; Zengerle, R.; Hoffmann, J. Fusing MEMS Technology with Lab-on-Chip: Nanoliter-Scale Silicon Microcavity Arrays for Digital DNA Quantification and Multiplex Testing. *Microsyst. Nanoeng.* **2020**, *6*, 328–341. [CrossRef]
18. Ren, Z.; Chang, Y.; Ma, Y.; Shih, K.; Dong, B.; Lee, C. Leveraging of MEMS Technologies for Otical Metamaterial Applications. *Adv. Opt. Mater.* **2020**, *8*, 1900653. [CrossRef]
19. Chircov, C.; Grumezescu, A.M. Microelectromechanical Systems (MEMS) for Biomedical Applications. *Micromachines* **2022**, *13*, 164. [CrossRef]
20. Alodhayb, A. Modeling of an Optically Heated MEMS-Based Micromechanical Bimaterial Sensor for Heat Capacitance Measurements of Single Biological Cells. *Sensors* **2020**, *20*, 215. [CrossRef]
21. Yu, Z.; Chen, S.; Mou, Y.; Hu, F. Electrostatic-Fluid-Structure 3D Numerical Simulation of MEMS Electrostatic Comb Resonator. *Sensors* **2022**, *22*, 1056. [CrossRef]
22. Wang, L.; Wang, C.; Wang, Y.; Quan, A.; Keshavarz, M.; Madeira, B.P.; Zhang, H.; Wang, C.; Kraft, M. A Review on Coupled Bulk Acoustic Wave MEMS Resonators. *Sensors* **2022**, *22*, 3857. [CrossRef]
23. Li, Y.; Li, H.; Xiao, Y.; Cao, L.; Guo, Z.S. A Compensation Method for Nonlinear Vibration of Silicon-Micro Resonant Sensor. *Sensors* **2021**, *21*, 2545. [CrossRef] [PubMed]
24. Vikas Garud, M.; Pratap, R. A Novel MEMS Speaker with Peripheral Electrostatic Actuation. *J. Microelectromech. Syst.* **2020**, *29*, 592–599. [CrossRef]
25. Arabi, M.; Alghamdi, M.; Kabel, K.; Labena, A.; Gado, W.S.; Mavani, B.; Scott, A.J.; Penlidis, A.; Yavuz, M.; Abdel-Rahman, E. Detection of Volatile Organic Compounds by Using MEMS Sensors. *Sensors* **2022**, *22*, 4102. [CrossRef] [PubMed]
26. Asher, A.; Gilat, R.; Krylov, S. Natural Frequencies and Modes of Electrostatically Actuated Curved Bell-Shaped Microplates. *Appl. Sci.* **2022**, *12*, 2704. [CrossRef]
27. Tunc, T.; Sarikaya, M.Z.; Yaldiz, H. Fractional Hermit Hadamard's Type Inequality for the Co-Ordinated Convex Function. *TWMS J. Pure Appl. Math.* **2020**, *11*, 3–29.
28. Noor, M.A.; Noor, K.I. Some New Classes of Strongly Generalized Preinvex Function. *TWMS J. Pure Appl. Math.* **2021**, *12*, 181–182.
29. Li, M.; Luo, A.; Luo, W.; Wang, F. Recent Progress on Mechanical Optimization of MEMS Electret-Based Electrostatic Vibration Energy Harvesters. *J. Microelectromech. Syst.* **2022**, *31*, 726–740. [CrossRef]
30. Mousavi, M.; Alzgool, M.; Lopez, D.; Towfighian, S. Open-Loop Control of Electrostatic Levitation Actuators to Enhance the Travel-Range of Optical Sqwitches. *Sens. Actuators A Phys.* **2022**, *338*, 113453. [CrossRef]
31. Williams, R.P.; Vatankhah, E.; Hall, N.A. Multidegree-of-Freedom State-Space Modeling of Nonlinear Pull-in Dynamics of an Electrostatic MEMS Microphone. *J. Microelectromech. Syst.* **2022**, *31*, 589–598. [CrossRef]
32. Alneamy, A.M.; Ouakad, H.M. Inertia Mass Bio-Sensors Based on Snap-Through Phenomena In Electrostatic MEMS Shallow Arch Resonator. *Int. J. Mech. Sci.* **2022**, *238*, 107825. [CrossRef]
33. Wang, Q.Y.; Zhang, L.; He, W.M.; Yang, L.; Zhang, C.; Wang, Z.Y.; Zhang, R.; Chen, J.H.; Wang, S.; Zang, S.Q.; et al. High-Performance Primary Explosives Derived From Copper Thiolate Cluster-Assembled Materials for Micro-Initiating Device. *Chem. Eng. J.* **2020**, *389*, 124455. [CrossRef]
34. Abozyd, S.; Toraya, A.; Gaber, N. Design and Modeling of Fiber-Free Optical MEMS Accelerometer Enabling 3D Measurements. *Micromachines* **2022**, *13*, 343. [CrossRef] [PubMed]
35. Lai, X.; Wang, Y.; Li, Q.; Habib, K. Reset Noise Sampling Feedforward Technique (RNSF) for Low Noise MEMS Capacitive Accelerometer. *Electronics* **2022**, *11*, 2693. [CrossRef]
36. Joshua, S.; Shokri, A.; Marian, D. Variable Step Hybrid Block Method for the Approximation of Kepler Problem. *Fractal Fract.* **2022**, *6*, 343.
37. Shokri, A.; Saadat, H. P-Stability, TF and VSDPL Technique in Obrechkoff Methods for the Numerical Solution of the Schroedinger Equation. *Bull. Iran. Math. Soc.* **2016**, *42*, 687–706.
38. Taussiff, M.; Ouakad, H.M.; Alqahtani, H. Global Nonlinear Dynamics of MEMS Arches Actuated by Fringing-Field Electrostatic Field. *Arab. J. Sci. Eng.* **2020**, *45*, 5959–5975. [CrossRef]
39. Da Costa, E.F.; De Oliveira, N.E.; Morais, F.J.O.; Carvalhaes-Dias, P.; Duarte, L.F.C.; Cabot, A.; Siqueira Dias, J.A. A Self-Powered and Autonomous Fringing Field Capacitive Sensor Integrated into a Micro Sprinkler Spinner to Measure Soil Water Content. *Sensors* **2017**, *17*, 575. [CrossRef]
40. Zaitsev, I.; Bereznychenko, V.; Bajaj, M.; Taha, I.B.M.; Belkhier, Y.; Titko, V.; Kamel, S. Calculation of Capacitive-Based Sensors of Rotating Shaft Vibration for Fault Diagnostic Systems of Powerful Generators. *Sensors* **2022**, *22*, 1634. [CrossRef]
41. Moheimani, R.; Gonzalez, M.; Dalir, H. An Integrated Nanocomposite Proximity Sensor: Machine Learning-Based Optimization, Simulation, and Experiment. *Nanomaterials* **2022**, *12*, 1269. [CrossRef]
42. Hu, W.; Wu, B.; Srivastava, S.K.; Ay, S.U. Comparative Study and Simulation of Capacitive Sensors in Microfluidic Channels for Sensitive Red Blood Cell Detection. *Micromachines* **2022**, *13*, 1654. [CrossRef]

43. Gua, K.; Laskar, N.M.; Gogoi, H.J.; Baishnab, K.L.; Rao, K.S. A New Analytical Model Switching Time of a Perforated MEMS Switch. *Microsyst. Technol.* **2020**, *26*, 3143–3152. [CrossRef]
44. Ghergu, M.; Miyamoto, Y. Radial Regular and Rupture Solutions for a MEMS Model wtih Fringing Field. *aXiv* **2020**, arXiv:2007.01406.
45. Petre, A.R.; Craciunescu, R.; Fratu, O. Design, Implementation and Simulation of a Fringing Field Capacitive Humidity Sensor. *Sensors* **2020**, *20*, 5644. [CrossRef] [PubMed]
46. Wei, J.; Ye, D. On MEMS Equation with Fringing Field. *Proc. Am. Math. Soc.* **2010**, *138*, 1693–1699. [CrossRef]
47. Di Barba, P.; Fattorusso, L.; Versaci, M. Curvature-Dependent Electrostatic Field as a Principle for Modelling Membrane MEMS device with Fringing Field. *Comput. Appl. Math.* **2021**, *40*, 87. [CrossRef]
48. Versaci, M.; Angiulli, G.; Fattorusso, L.; Jannelli, A. On the Uniqueness of the Solution for a Semi-Linear Elliptic Boundary Value Problem of the Membrane MEMS Device for Reconstructing the Membrane Profile in Absence of Ghost Solutions. *Int. J. Non-Linear Mech.* **2019**, *109*, 24–31. [CrossRef]
49. Versaci, M.; Angiulli, G.; Jannelli, A. Recovering of the Membrane Profile of an Electrostatic Circular MEMS by a Three-Stage Lobatto Procedure: A Convergence Analysis in the Absence of Ghost Solutions. *Mathematics* **2020**, *8*, 487. [CrossRef]
50. Cassani, D.; Fattorusso, L.; Tarsia, A. Global Existence for Nonlocal MEMS. *Nonlinear Anal.* **2011**, *74*, 5722–5726. [CrossRef]
51. Di Barba, P.; Versaci, M. Deformable MEMS with Fringing Field: Models, Uniqueness Conditions and Membrane Profile Recovering. *Electronics* **2022**, *11*, 798.
52. Cassani, D.; Fattorusso, L.; Tarsia, A. Nonlocal Dynamic Problems with Singular Nonlinearities and Applications to MEMS. *Anal. Topol. Nonlinear Differ. Equ.* **2014**, *85*, 187–206.
53. Miyasita, T. Convergence of Solutions of a Nonlocal Biharmonic MEMS Equation with the Fringing Field. *J. Math. Anal. Appl.* **2017**, *454*, 265–284. [CrossRef]
54. Hou, D.; Wang, H.; Zhang, C. Positivity-Preserving and Unconditionally Energy Stable Numerical Schemes for MEMS model. *Appl. Numer. Math.* **2022**, *181*, 503–517. [CrossRef]
55. Guerra, I. A semilinear problem with a gradient term in the nonlinearity. *Discret. Contin. Dyn. Syst.* **2022**, *42*, 137–162. [CrossRef]
56. Miyasita, T. On a Nonlocal Biharmonic MEMS Equation with the Navier Boundary Condition. *Sci. Math. Jpn.* **2017**, *80*, 189–208.
57. Lin, F.; Yang, Y. Nonlinear Non-local Elliptic Equation Modelling Electrostatic Actuator. *Proc. R. Soc. Math. Phys. Eng. Sci.* **2007**, *463*. [CrossRef]
58. Campanato, S. *Sistemi Ellittici in Forma Divergenza: Regolaritá all'Interno*; Scuola Normale Superiore di Pisa: Pisa, Italy, 1980.
59. Pelesko, J.A.; Triolo, A.A. Nonlocal Problems in MEMS Device Control. *J. Eng. Math.* **2001**, *41*, 345–366. [CrossRef]
60. Cassani, D.; d'O, J.M.; Ghoussoub, N. On a Fourth Order Elliptic Problem with a Singular Nonlinearity. *Adv. Nonlinear Stud.* **2011**, *9*, 189–209. [CrossRef]
61. Tarsia, A. Differential Equations and Implicit Functions: A Generalization of the Near Operator Theorem. *Topol. Methods Nonlinear Anal.* **1998**, *11*, 115–133. [CrossRef]
62. Girbau, D.; Lazaro, A.; Pradell, L. Characterization of dynamics and power handling of RF MEMS using vector measurement techniques. *IEEE Trans. Microw. Theory Tech.* **2004**, *52*, 2627–2633. [CrossRef]
63. de Groot, W.A.; Webster, J.R.; Felnhofer, D.; Gusev, E.P. Review of Device and Reliability Physics of Dielectrics in Electrostatically Driven MEMS Devices. *IEEE Trans. Device Mater. Reliab.* **2009**, *9*, 190–202. [CrossRef]